PROTEINS: Structure, Function, and Bioinformatics 63:1127–1131 (2006)

STRUCTURE NOTE

Crystal Structure of Human Spermidine/Spermine N^1-Acetyltransferase (hSSAT): The First Structure of a New Sequence Family of Transferase Homologous Superfamily

Yong-Qun Zhu,[1,2] De-Yu Zhu,[1,2] Lei Yin,[1,2] Ying Zhang,[1] Clemens Vonrhein,[3] and Da-Cheng Wang[1]*

[1]*National Laboratory of Biomacromolecules, Institute of Biophysics, Chinese Academy of Sciences, Beijing, People's Republic of China*

[2]*Graduate School of the Chinese Academy of Sciences, Beijing, People's Republic of China*

[3]*Global Phasing Ltd., Sheraton House, Castle Park, Cambridge, England*

Introduction. Polyamines including putrescine, spermidine, and spermine are important polycationic small molecules for life. They are involved in protein synthesis, cell growth, and regulation of several metabolic processes in a cell.[1] Overaccumulation of the polyamines is toxic to cells. The intracellular concentration of polyamines is carefully controlled by a combination of regulated enzymatic steps, including biosynthetic enzymes such as ornithine decarboxylase, and catabolic enzymes such as spermidine/spermine N^1-acetyltransferase (SSAT).[2,3]

SSAT is one of the diamine *N*-acetyltransferases and a rate-limiting enzyme, which has a key role in polyamine metabolism. It catalyzes the N^1-acetylation of spermine and spermidine to form less charged derivatives that are either excreted from the cell or undergo further metabolism. It is the turning point of the polyamine metabolism pathway.[4] So far 11 proteins have been identified as belonging to the SSAT homologous family, as shown in Figure 1. Although the function of SSAT is important, the three-dimensional structure as well as the mechanism of enzyme reaction and actual activity site of SSAT are still unknown.

Human SSAT (hSSAT), containing 171 residues, is related with many serious diseases, such as human colon cancer and infection of human immunodeficiency virus-1.[5,6] Herein, we report the crystal structure of hSSAT, which is the first structure of diamine *N*-acetyltransferases. The fold of hSSAT belongs to the transferase homologous superfamily. The comparisons of sequence and structure show that the hSSAT structure is the representative of a new sequence family of transferase superfamily. Three-dimensional structure also suggests the potential enzyme activity site of hSSAT.

Materials and Methods. *Cloning, expression, and purification.* Polymerase chain reaction primers, including NdeI and XhoI restriction sites, were designed to amplify the *hSSAT* gene (GenBank: NP_002961) from reverse transcriptase-polymerase chain reaction products of human hemopoietic stem cell. The gene was inserted into the pET22b(+) vector (Novagen), and the recombinant protein was overexpressed as a C-terminal His-tagged protein in *Escherichia coli* BL21(DE3). The cells were grown in LB at 37°C and induced with 1 mM IPTG when the culture reached an $O.D_{600}$ of 0.6–0.8. The harvested cells were resuspended in the lysis buffer (50 mM NaH_2PO_4, pH8.0; 300 mM NaCl; 10 mM imidazole) with 0.1 mM PMSF and sonicated. The lysate was centrifuged at 15,000 revolutions per minute (rpm) at 4°C for 20 min. The supernatant was loaded directly into a Ni-NTA column (Novagen) preequilibrated with lysis buffer. Then the column was washed with wash buffer (50 mM NaH_2PO_4, pH8.0; 300 mM NaCl; 20 mM imidazole) and the target protein was eluted with elution buffer (50 mM NaH_2PO_4, pH 8.0; 300 mM NaCl; 250 mM imidazole). The eluate was concentrated by ultrafiltration (Millipore) and then loaded into a Superdex75 HR16/60 column (Amersham Pharmacia) preequilibrated with buffer of 20 mM Tris-HCl pH 8.0 at 16°C. Further purification was performed with a global Mono Q HR5/5 (Amersham Pharmacia). Finally, hSSAT was desalted with the buffer of 20 mM Tris-HCl pH 8.0. The purified protein was analyzed using sodium dodecyl sulfate-polyacrylamide gel electrophoresis.

Crystallization. The purified protein was concentrated to 50 mg/mL for crystallization. Crystallization experiments were performed with the hanging-drop vapor-diffusion method combined with micro-seeding at 20°C. The diffusion drops were formed with 1 μL of protein solution and 1 μL of reservoir solution and seeded immediately. Then the drops were equilibrated against 0.5 mL of reservoir solu-

Grant sponsors: Ministry of Science and Technology of China and Chinese Academy of Sciences; Grant numbers: KSCX1-SW-17, KSCX2-SW-322.

*Correspondence to: Da-Cheng Wang, National Laboratory of Biomacromolecules, Institute of Biophysics, Chinese Academy of Sciences, No. 15 Datun Road, Beijing 100101, People's Republic of China. E-mail: dcwang@sun5.ibp.ac.cn

Received 7 December 2005; Accepted 11 January 2006

Published online 16 March 2006 in Wiley InterScience (www.interscience.wiley.com). DOI: 10.1002/prot.20965

© 2006 WILEY-LISS, INC.

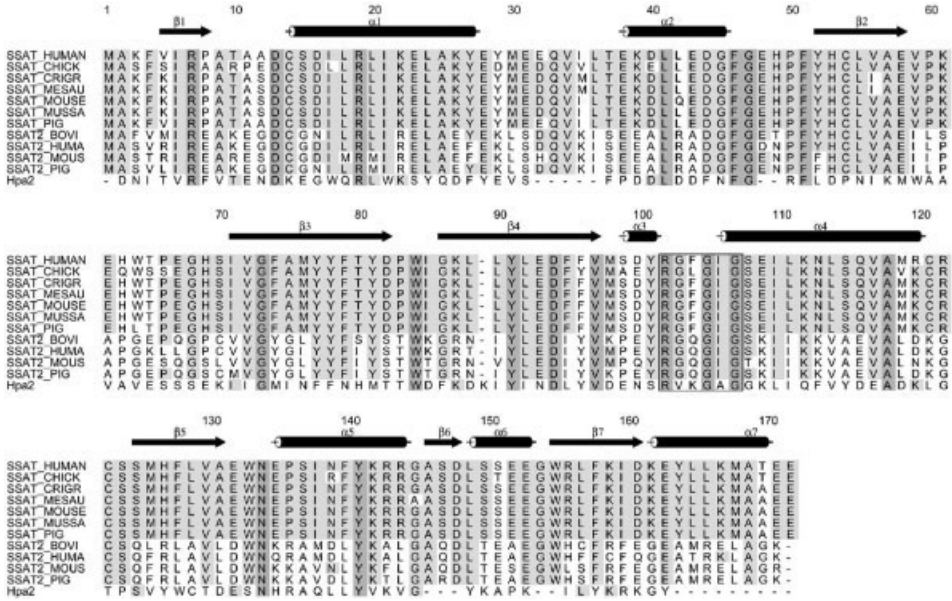

Fig. 1. Secondary structure of hSSAT and sequence alignment between SSAT proteins and Hpa2. SSAT = spermidine/spermine N^1-acetyltransferase. Hpa2 is the histone acetyltransferase from yeast. The secondary-structure elements (β-sheet, α-helix) found in hSSAT are shown above the sequence. The identical and homologous residues are shaded in dark gray and light gray, respectively. The consensus sequence for the acetyl CoA binding site is highlighted by box. Eleven aligned SSAT homologous proteins were obtained from UniProt.[21] The sequence alignment was performed with ClustalW[22] and the figure was prepared with ALSCRIPT.[23]

tion containing 2.6 M NaCl, 0.1 M Tris-HCl pH 8.0, and 0.1 M potassium sodium tartrate. The qualified crystals suitable for X-ray diffraction were obtained after one night.

Data collection and processing. All diffraction data were collected on a Rigaku FRE diffraction system using a Rigaku R-Axis IV++ image plate detector. For preparation of the iodine-derivative crystals, quick-soaking method was used. The crystal was soaked in the heavy-atom soaking solution (2.6 M NaCl, 0.1 M Tris-HCl, 0.1 M potassium sodium tartrate and 0.5 M KI) for 30 s before mounting the crystal. Native crystal was soaked the same way using native-soak solution (2.6 M NaCl, 0.1 M Tris-HCl pH 8.0, and 0.1 M potassium sodium tartrate) to maintain the same isomorph. Then the crystals were flash-cooled in the nitrogen-gas stream at 95 K. Two sets of data were collected with the crystal-to-detector distance of 220 mm and exposed for 3 min with 1° oscillation per frame. The iodine-derivative data were collected to 360 frames and native data to 107 frames. MOSFLM, SCALA, and TRUNCATE from the CCP4 program suite[7] were used for processing, reduction, and scaling of the diffraction data. Data statistics are summarized in Table I.

Structure determination and refinement. The structure of hSSAT was successfully determined through the iodine short-cryo soaking approach.[8] The program SHELXD was used to search initial iodine atom sites. The iodine atom sites were detected again and refined by SHARP[9] using isomorphous and anomalous signals. There are 22 iodine sites found in an asymmetric unit. After initial phasing by SHARP and density modification by SOLOMON, further density modification was performed with DM[10] (average) from the CCP4 program suit[7] to refine the phase. The initial model consisting of 70% of the hSSAT structure was built automatically by using ARP/wARP.[7,11] The remainder of the model was manually built using O.[12] The structure was refined to the resolution of 2.3 Å with CNS version 1.1.[13] The final model was built up with R-factor of 0.201 and R_{free} of 0.269. The quality of the structure was checked using PROCHECK.[14] The statistics are listed in Table I.

Results and Discussion. The final structure model of hSSAT contains two protein molecules (residues 3–169 for chain A, residues 3–170 for chain B) and 359 water molecules. The whole hSSAT sequence has 171 residues. Because of lack of electron density, seven residues at N- and C-terminal, including A1, A2, A170, A171, and B1, B2, B171, are missed. The His-tag at C-terminal also does not appear in the electron density map. Two residues (Glu-B48 and Glu-B67) are in disallowed regions of the Ramachandran plot, which are well defined by the clear density maps. At the moment, there is no special reason to be found for these strained conformations.

There are two hSSAT molecules related by a noncrystallographic twofold axis in the asymmetric unit, which are integrated into a stable dimer via a unique way [Fig. 2(a)]. The tertiary structure of the hSSAT monomeric partner adopts a compact α/β fold mode, which consists of seven β-strands which consists of seven β-strands (β_1–β_7) connected by six α-helices (α_1–α_2, α_4–α_7) and a 3_{10} helix (α_3) [Fig. 2(b)]. The core structure of monomer contains a central five-stranded antiparallel β-sheet (β_1–β_5) and four

TABLE I. Data Collection, Phasing, and Structure Refinement Statistics of hSSAT

	Native	KI-derivate
A. Data collection		
Space group	$P4_3$	$P4_3$
Molecules/ASU	2	2
a (Å)	46.336	46.358
b (Å)	46.336	46.358
c (Å)	180.489	178.878
Wavelength (Å)	1.5418	1.5418
Resolution range (Å)	40–2.30	40–2.4
Observation (I/σ (I) > 0)	59925	152246
Unique reflections (I/σ (I) > 0)	15,954	14,135
Last shell (Å)	2.36–2.30	2.46–2.40
R_{sym} (%)[a]: overall (last shell)	0.052 (0.115)	0.078 (0.509)
$\langle I/\sigma(I)\rangle$: overall (last shell)	18.9 (6.7)	28.5 (3.1)
Completeness (%): overall (last shell)	95.2 (72.8)	94.9 (78.6)
Redundancy: overall (last shell)	3.8 (1.8)	10.8 (6.2)
B. Phasing		
Iodine atom sites		22
Resolution range of data used		25.2–2.4
Phasing power	iso	ano
	0.88	0.86
FOM	0.25	
FOM after SOLOMON	0.73	
FOM after DM (average)	0.87	
C. Structure refinement		
Resolution range (Å)	25.2–2.30	
Sigma cutoff	0.0	
R-factor	0.201	
R_{free}[b]	0.269	
Ramachandran statistics (%)[c]		
Most favored regions	88.6	
Additionally allowed regions	10	
Generously allowed regions	0.7	
Disallowed regions	0.7	

[a] $R_{sym} = \Sigma(|I| - |\langle I\rangle|)/\Sigma|I|$.
[b] R_{free} calculated using 10% of total reflections omitted from refinement.
[c] Ramachandran statistics calculated using PROCHECK.[14]

helices (α_1–α_4). The helices of α_1 and α_2 connect strands β_1 and β_2 and are located on the convex face of this five-stranded antiparallel β-sheet, whereas the helices of α_3 and α_4, which connect strands β_4 and β_5, are located on the concave face. It is interesting that the remaining structural elements at the C-terminal, including α_5, β_6, α_6, β_7, and α_7, are rather separately arranged out of the core structure to form a long tail of the tertiary structure [Fig. 2(b)]. Evidently, this separated C-terminal segment needs to be stabilized by special structural factors. Actually, this special structural requirement is notably satisfied by the dimerization of two hSSAT molecules. In the dimeric form of hSSAT, the long β-strand at C-terminal, β_7 of one molecule, is subtly inserted into the space between β_5 and β_6 of the partner molecule to form a heterogeneous three-stranded antiparallel β-sheet through 11 pairs of intermolecular main-chain hydrogen bonds (eight between residues 123–131 of Mol A and residues 153–161 of Mol B and three between residues 146–149 of Mol A and residues 158–156 of Mol B) [Fig. 2(c)]. This heterogeneous three-stranded β-sheet is further combined with β_1–β_4 to construct an integrated seven-stranded antiparallel β-sheet as a more stable molecular scaffold for hSSAT monomer. By accompanying, the C-terminal helix α_7 of one molecule is also moved and stabilized by interacting with helix α_4 of the partner molecule [Fig. 2(c)]. We refer to this unique way for the dimerization of hSSAT as C-terminal exchange. Through C-terminal exchange, two hSSAT molecules are firmly assembled to an intact dimer, which is the main structural character of hSSAT. It implies that the dimeric form of hSSAT is its basic structural and functional unit. In fact, our experiment data showed that hSSAT is really a dimer in solution (data not shown here).

The structure similarity search with Dali revealed that the core fold of hSSAT, consisting of six strands with four surrounding α-helices, is generally consistent with the typical transferase fold in CATH,[15,16] in which the protein domain structures are hierarchically classified. Through analysis with the combinatorial extension (CE),[17] all of the structures similar to hSSAT belong to the transferase family. So it strongly identified that hSSAT belongs to the transferase homologous superfamily (CATH code: 3.40.630.30). So far, there are 22 sequence families found in the transferase homologous superfamily. The PSI-BLAST[18] result indicates that there is no obvious sequence similarity between hSSAT and all other structures of the transferase homologous family. Further sequence comparison was performed with SSAP.[19] It indicates that hSSAT has less than 20% sequence identity to each representative member of 22 sequence families. According to CATH criteria of S-level classification, hSSAT should be assigned to a new sequence family of the transferase homologous superfamily.

The structural comparisons showed that the closest structural homolog of hSSAT was the histone acetyltransferase Hpa2[20] from yeast (Hpa2, PDB ID 1QSM; SSAP score, 85.03%, overlap, 88%; root-mean-square deviation, 2.47 Å for equivalent 147 aligned residues). However, there is only 16% sequence identity between hSSAT and Hpa2. The main structure difference between these two structures is located at the C-terminal segment where hSSAT has an additional α helix (α_7). Hpa2 is a member of the Gcn5-related *N*-acetyltransferase (GNAT) family. It has a conserved acetyl CoA binding site, which is characterized with the sequence of RXXGXG (X can be any amino acid residue).[20] This characterized sequence is also conserved in 11 proteins of the SSAT family (residues 101–106 with sequence RGFGIG) (Fig. 1). The structural comparison between hSSAT and Hpa2-acetyl CoA complex showed that hSSAT has a similar tertiary structure at this acetyl CoA binding site. It indicates that hSSAT should adopt a similar acetyl CoA binding site and activity site as Hpa2.

The hSSAT is the first structure of diamine *N*-acetyltransferases and the SSAT homologous family. So far, the detailed mechanism of bioactivity of hSSAT is still in question. The tertiary structure of hSSAT reported in this article provides a sound basis for the in-depth study of its structure–function relationship.

Protein Data Bank Accession Code. Coordinates and structure factors for the structure of hSSAT have been deposited at the Protein Data Bank with accession code 2F5I.

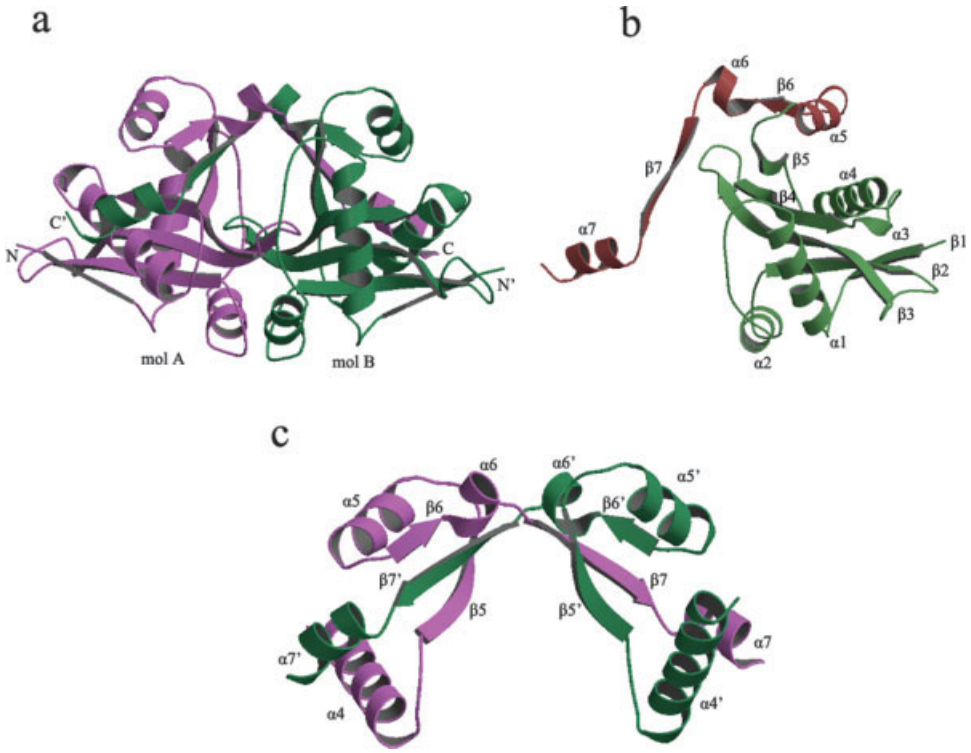

Fig. 2. **a:** Ribbon diagram of hSSAT dimer. Ribbons are colored in orchid and green for molecule A and B, respectively. Two molecules are related by a noncrystallographic twofold axis. **b:** Diagram of hSSAT monomer structure. β_1–β_5 and α_1–α_4 as the core structure are shown in green. The separated C-tail of the molecule consisting of β_6–β_7 and α_5–α_7 is shown in red. The β_7-strand from the opposite molecule will be inserted into the space between β_5 and β_6 in dimeric form. **c:** C-terminal exchange and interaction segments in hSSAT dimer. α_4–α_7 and β_5–β_7 are from molecule A (orchid). α_4'–α_7' and β_5'–β_7' are from opposite molecule B (green). In dimerization, the strand β_7 at the C-terminal of A is inserted into the space between β_5' and β_6' of B to form a heterogeneous three-stranded β-sheet, which will further contact the sheet of β_1'–β_4' to build up a more stable molecular scaffold (shown in a and b). By accompanying, the C-terminal helix α_7 of molecule A is moved to contact with α_4' of molecule B. The figures were prepared using Molscript.[24]

Acknowledgments. The X-ray data collection was supported by the Photon Factory at KEK (20005G253), Japan. The authors thank Yi Han of the protein platform of Institute of Biophysics for providing the X-ray facility in house for crystallographic analysis and data collection.

REFERENCES

1. Kaasinen SK, Oksman M, Alhonen L, Tanila H, Janne J. Spermidine/spermine N1-acetyltransferase overexpression in mice induces hypoactivity and spatial learning impairment. Pharmacol Biochem Behav 2004;78(1):35–45.
2. Seiler N. Functions of polyamine acetylation. Can. J Physiol Pharmacol 1987;65:2024–2035.
3. Bordin L, Vargiu C, Colombatto S, et al. Casein kinase 2 phosphorylates recombinant human spermidine/spermine N1-acetyltransferase on both serine and threonine residues. Biochem Biophys Res Commun 1996;229(3):845–851.
4. Casero RA, Pegg AE. Spermidine/spermine N1-acetyltransferase: the turning point in polyamine metabolism. FASEB J 1993;7:653–661.
5. Babbar N, Ignatenko NA, Casero RA Jr, Gerner EW. Cyclooxygenase-independent induction of apoptosis by sulindac sulfone is mediated by polyamines in colon cancer. J Biol Chem 2003;278 (48):47762–47775.
6. Lake JA, Carr J, Feng F, Mundy L, Burrell C, Li P. The role of Vif during HIV-1 infection: interaction with novel host cellular factors. J Clin Virol 2003;26(2):143–152.
7. Collaborative Computational Project, Number 4. The CCP4 suite: programs for protein crystallography. Acta Crystallogr D Biol Crystallogr 1994;50:760–763.
8. Dauter Z, Dauter M, Rajashankar KR. Novel approach to phasing proteins: derivatization by short cryo-soaking with halides. Acta Crystallogr D Biol Crystallogr 2000;D56:232–237.
9. De La Fortelle E, Bricogne G. Maximum-likelihood heavy-atom parameter refinement in the MIR and MAD methods. In: Sweet RM, Carter CW, editors. Methods in Enzymology, Macromolecular Crystallography. New York: Academic Press; 1997. 276:472–494.
10. Cowtan K. Joint CCP4 and ESF-EACBM Newsletter on Protein Crystallography. 1994;31:34–38.
11. Morris RJ, Perrakis A, Lamzin VS. ARP/wARP and automatic interpretation of protein electron density maps. Methods Enzymol 2003;374:229–244.
12. Jones TA, Zou JY, Cowan SW, Kjeldgaard M. Improved methods for building protein models in electron density maps and the location of errors in these models. Acta Crystallogr A 1991;47:110–119.
13. Brünger AT, Adams PD, Clore GM, et al. Crystallography & NMR system: a new software suite for macromolecular structure determination. Acta Crystallogr D Biol Crystallogr 1998;54: 905–921.
14. Laskowski RA, MacArthur MW, Moss DS, Thornton JM. PROCHECK: a program to check the stereochemical quality of protein structures. J Appl Crystallogr 1993;26:283–291.
15. Orengo CA, Michie AD, Jones S, Jones DT, Swindells MB, Thornton JM. CATH: a hierarchic classification of protein domain structures. Structure 1997;5(8):1093–1108.
16. Pearl FM, Bennett CF, Bray JE, et al. The CATH database: an

extended protein family resource for structural and functional genomics. Nucleic Acids Res 2003;31:452–455.
17. Shindyalov IN, Bourne PE. Protein structure alignment by incremental combinatorial extension (CE) of the optional path. Protein Eng 1998;11(9):739–747.
18. Altschul SF, Madden TL, Schaffer AA, et al. Gapped BLAST and PSI-BLAST: a new generation of protein database search programs. Nucleic Acids Res 1997;25:3389–3402.
19. Orengo CA, Taylor WR. SSAP: sequential structure alignment program for protein structure comparison. Methods Enzymol 1996;266:617–635.
20. Angus-Hill ML, Dutnall RN, Tafrov ST, Sternglanz R, Ramakrishnan V. Crystal structure of the histone acetyltransferase Hpa2: a tetrameric member of the Gcn5-related N-acetyltransferase superfamily. J Mol Biol 1999;294:1311–1325.
21. Bairoch A, Apweiler R, Wu CH, et al. The Universal Protein Resource (UniProt). Nucleic Acids Res 2005;33:D154–159.
22. Thompson JD, Higgins DG, Gibson TJ. CLUSTAL W: improving the sensitivity of progressive multiple sequence alignment through sequence weighting, position-specific gap penalties and weight matrix choice. Nucleic Acids Res 1994;22:4673–4680.
23. Barton GJ. ALSCRIPT: a tool to format multiple sequence alignments. Protein Eng 1993;6:37–40.
24. Kraulis PJ. MOLSCRIPT: a program to produce both detailed and schematic plots of protein structures. J Appl Crystallogr 1991;24:946–950.